2012 International Conference on Image, Vision and Computing (ICIVC 2012)
IPCSIT vol. 50 (2012) © (2012) IACSIT Press, Singapore
DOI: 10.7763/IPCSIT.2012.V50.61

Frequency-Domain Study of Lock Range of Injection-Locked Non-Harmonic Oscillators

Yushi Zhou and Fei Yuan[1]

Department of Electrical and Computer Engineering
Ryerson University, Toronto, Ontario, Canada

Abstract: This paper investigates the lock range of injection-locked non-harmonic oscillators using a frequency-domain approach. By representing a non-harmonic oscillator with a set of harmonic oscillators, the intrinsic relation between the lock range of the harmonic oscillators and that of the non-harmonic is obtained. We show that non-harmonic oscillators exhibit a larger lock range as compared with harmonic oscillators. We further show that non-harmonic oscillators with a multi-tone injection exhibit a larger lock range as compared with that with a single-tone injection. The theoretical findings are verified using a sub-threshold relaxation oscillator designed in IBM 130 nm 1.2 V CMOS technology.

Keywords: Non-Harmonic Oscillators, Harmonic Oscillators, Injection-Locking.

1. Introduction

Non-harmonic oscillators such as relaxation oscillators and ring oscillators have been widely used in passive wireless microsystems such as as RFID (radio-frequency identification) systems, passive wireless sensors, and biomedical implants [1]. Arising from process spread, supply voltage fluctuation, and temperature variation, the frequency of these oscillator exhibits a high degree of uncertainty. The uncertainty of the frequency of the system clock of passive wireless microsystems is further escalated by the fact that these systems are usually fabricated using low-cost CMOS technologies, which typically have a high degree of process spread. Since the operation of the baseband units of a passive wireless microsystem and the up-link from the microsystem to its base station are controlled by its system clock, a stringent requirement on the frequency of the system clock exists. For example, EPC radio-frequency identity protocols class-1 generation-2 UHF RFID protocols require that the accuracy of the frequency of the backscattered data be upper-bounded by ±4% [2]. Remote calibration of the system clock of passive wireless microsystems from their base station is critical. Injection-locking has been demonstrated to be a power-efficient means for remote frequency calibration of passive wireless microsystems [3]. The success of injection-locking based remote frequency calibration is largely affected by the lock range of these non-harmonic oscillators. Ultra low-power non-harmonic oscillators with a large lock range are highly desirable in these applications. Using a phaser-domain approach, Razavi showed that the lock range of a harmonic oscillator in weak injection is given by [4]

$$|\Delta\omega| = \frac{\omega_o}{2Q}\frac{I_{inj}}{I_{osc}} \tag{1}$$

where I_{inj} and I_{osc} are the amplitude of the injection current and that of the LC tank current, respectively, ω_o and Q are the resonance frequency and quality factor of the LC tank, respectively. Revealed by (1) is that the lock range is directly proportional to the strength of the injection signal and inversely proportional to the

[1] Corresponding author: Fei Yuan. Tel. (416) 979-5334. Fax: (416) 979-5280.
Email: fyuan@ee.ryerson.ca

quality factor of the LC tank. Increasing the amplitude of injection signal I_{inj}, though increasing the lock range, is at the cost of power consumption. Harmonic oscillators, such as LC-tank oscillators, typically exhibit better phase noise performance as compared with non-harmonic oscillators because of its relative high quality factor given by [5].

$$S_y(\omega) = \frac{1}{4Q^2}\left(\frac{\omega_o}{\Delta\omega}\right)^2 S_x(\omega) \tag{2}$$

The lock range of harmonic oscillators, however, is smaller mainly due to the narrow-band characteristics of the LC tanks of these oscillators. In addition, the injection-induced impedance variation of these oscillators, which is one of the key factors determining the lock range, is also smaller as compared with that of non-harmonic oscillators [6]. A phasor domain model of the lock range of harmonic oscillators was given in [7]. Maffezzoni [8] proposed a mathematical model to predict the synchronization region of strongly nonlinear oscillators. An in-depth mathematical treatment of lock range of non-harmonic oscillators, and their intrinsic relation with that of harmonic oscillators in the frequency domain, however, are not available. This paper presents a general frequency-domain approach to analyze the lock range of non-harmonic oscillators. Using the definition of the open-loop quality factor of harmonic oscillators introduced by Razavi [5]

$$Q = \frac{\omega_o}{2}\sqrt{\left[\frac{\partial A}{\partial \omega}\right]^2 + \left[\frac{\partial \phi}{\partial \omega}\right]^2}\,, \tag{3}$$

where $H_o = Ae^{j\phi}$ is the loop gain of the oscillator, we show that non-harmonic oscillators exhibit a larger lock range as compared with their harmonic counterparts. We further show that the lock time of non-harmonic oscillators with a multi-tone injection is smaller as compared with that of non-harmonic oscillators with a single-tone injection. The theoretical findings are verified using a sub-threshold relaxation oscillator designed in IBM 130 nm 1.2 V CMOS technology.

2. Lock Range

A distinct characteristic of non-harmonic oscillators is their square-wave-like output waveform. To capture the essence of non-harmonic oscillators, we assume that the waveform of non-harmonic oscillators is a purely square wave such that it can be represented by a Fourier series with fundamental frequency $\omega_o = 2\pi/T_o$ where T_o is the frequency of the oscillator. If the waveform of the output of the oscillator is shown in Fig.1(a), its spectrum will only contain the fundamental and odd harmonics. Since the spectrum of the oscillator consists of a train of impulses at $\omega_o, 3\omega_o, 5\omega_o$,..., the oscillator can be considered as the assembly of a set of ideal harmonic oscillators that oscillate at $\omega_o, 3\omega_o, 5\omega_o$, ..., respectively. Each harmonic oscillator can be represented by a feedback system that satisfies Barkhausen oscillation criteria. When the noise and loss of the oscillator are considered, the square waveform of the output of the non-harmonic oscillator is replaced with the skirt-like waveform, as shown in Fig.1(b).

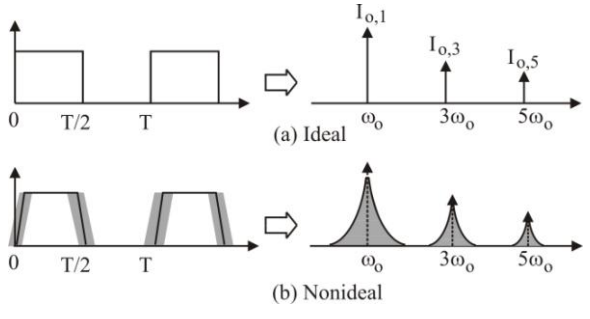

Figure 1: Time-domain waveform and spectrum of non-harmonic oscillators

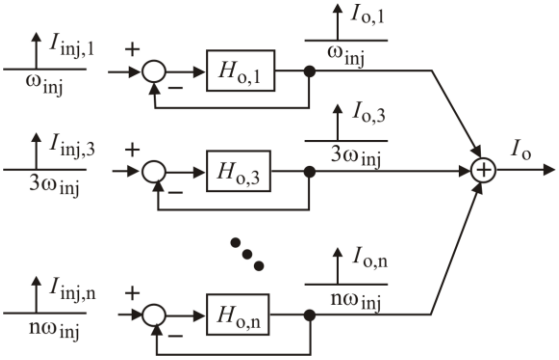

Figure 2: Representation of injection-locked non-harmonic oscillators with injection-locked harmonic oscillators.

The output of the non-harmonic oscillator can be denoted as

$$I_o = I_{o,1}\delta(\omega - \omega_o) + I_{o,3}\delta(\omega - 3\omega_o) + \ldots, \tag{4}$$

where $I_{o,n} = H_{o,n}/(1+H_{o,n})I_{inj,n}$ and $\delta(\omega)$ is discrete Dirac function depicting the multi-frequency nature of the spectrum of $I_o(t)$. Note that $\delta(\omega)=1$if $\omega=0$ and 0 otherwise.When an injection signal $I_{inj}(t)$ is within the lock range of a non-harmonic oscillator, the frequency of the oscillator will be shifted to that of the injection signal in the lock state. If $I_{inj}(t)$ is a single-tone at ω_{inj} , it can be represented by $I_{inj}(t) = I_{inj}\delta(\omega-\omega_{inj})$. Since the output of the oscillator is a multi-tone, $I_{inj}(t)$ will affect the input of the harmonic oscillators representing the non-harmonic oscillator. The inputs of the harmonic oscillators are denoted by $I_{inj,11}$, $I_{inj,31}$,..., $I_{inj,m1}$,..., where the sub-index m identifies m^{th} harmonic oscillator and the sub-index "1" signifies the single-tone input at ω_{inj}, as illustrated graphically in Fig.2. If I_{inj} is a multi-tone, such as a square wave, it can be represented by

$$I_{inj}(t) = I_{inj,1}\delta(\omega-\omega_{inj}) + I_{inj,3}\delta(\omega-3\omega_{inj}) + \ldots \tag{5}$$

Both the fundamental and harmonic components of $I_{inj}(t)$ will affect the inputs of the harmonic oscillators. The contribution of $I_{inj,1}$ to the input of the 1st, 3rd, 5th, ..., harmonic oscillators is represented by $I_{inj,11}$, $I_{inj,31}$, $I_{inj,51}$, ..., respectively. Similar notation applies to other harmonics oscillators as well. Let us assume that the injection signal $I_{inj}(t)$ causes the fundamental frequency of a non-harmonic oscillator to shift from ω_o to $\omega_o + \Delta\omega_o$ with $\Delta\omega_o << \omega_o$ in the lock state. The loop gain of nth harmonic oscillator can be represented by

$$H_{o,n}(n\omega_o + n\Delta\omega_o) = H_{o,n}(n\omega_o) + \left[\frac{\partial H_{o,n}}{\partial\omega}\right]_{n\omega_o}(n\Delta\omega). \tag{6}$$

Therefore

$$\left[\frac{\partial H_{o,n}}{\partial\omega}\frac{\partial H^*_{o,n}}{\partial\omega}\right]_{n\omega_o} = \left(\frac{\partial A_n}{\partial\omega}\right)^2_{n\omega_o} + \left(\frac{\partial\phi_n}{\partial\omega}\right)^2_{n\omega_o}, \tag{7}$$

where $H_{o,n} = A_n e^{j\phi_n}$ is the loop gain of n^{th} harmonic oscillator and * denotes the complex conjugate operator. Noting that $1+A_n(n\omega_o)=0$ at $\omega=n\omega_o$. Extend Razavi's definition of the open-loop quality factor of harmonic oscillators to n^{th} harmonic oscillator

$$Q_n = \frac{n\omega_o}{2}\sqrt{\left[\frac{\partial A_n}{\partial\omega}\right]^2_{n\omega_o} + \left[\frac{\partial\phi_n}{\partial\omega}\right]^2_{n\omega_o}}. \tag{8}$$

Eq.(7) becomes

$$\left[\frac{\partial H_{o,n}}{\partial\omega}\frac{\partial H^*_{o,n}}{\partial\omega}\right]_{n\omega_o} = \left(\frac{2Q_n}{n\omega_o}\right)^2. \tag{9}$$

Consider a single-tone injection signal at $\omega=\omega_{inj}$. Let the inputs to 1st, 3rd, 5th,..., harmonic oscillators be $I_{inj,11}$, $I_{inj,31}$, $I_{inj,51}$,..., respectively. The output of the oscillator is obtained from

$$I_o = \frac{H_{o,1}(\omega+\Delta\omega)}{1+H_{o,1}(\omega+\Delta\omega)}I_{inj,11}\delta(\omega-\omega_{inj}) + \frac{H_{o,3}(\omega+3\Delta\omega)}{1+H_{o,3}(\omega+3\Delta\omega)}I_{inj,31}\delta(\omega-3\omega_{inj}) + \ldots \tag{10}$$

Using the first-order Taylor approximation, Eq.(10) becomes

$$I_o = \frac{-I_{inj,11}\delta(\omega-\omega_{inj})}{\left[\frac{\partial H_{o,1}}{\partial\omega}\right]_{\omega_o}\Delta\omega} + \frac{-I_{inj,31}\delta(\omega-3\omega_{inj})}{\left[\frac{\partial H_{o,3}}{\partial\omega}\right]_{3\omega_o}(3\Delta\omega)} + \ldots. \tag{11}$$

Because $\delta(\omega-\omega_i)\delta(\omega-\omega_j)=1$if $i=j$ and 0 otherwise, it follows from (11)

$$I_o I_o^* = \frac{I^2_{inj,11}\delta(\omega-\omega_{inj})}{\left[\frac{\partial H_{o,1}}{\partial\omega}\frac{\partial H^*_{o,1}}{\partial\omega}\right]_{\omega_o}(\Delta\omega)^2} + \frac{I^2_{inj,31}\delta(\omega-3\omega_{inj})}{\left[\frac{\partial H_{o,3}}{\partial\omega}\frac{\partial H^*_{o,3}}{\partial\omega}\right]_{3\omega_o}(3\Delta\omega)^2} + \ldots. \tag{12}$$

Utilizing (9) derived earlier and matching the components that have the same frequency in (12) yield

$$I_{o,1}^2 = \left(\frac{\omega_o}{2Q_1}\right)^2 \frac{1}{(\Delta\omega)^2} I_{inj,11}^2,$$

$$I_{o,3}^2 = \left(\frac{\omega_o}{2Q_3}\right)^2 \frac{1}{(\Delta\omega)^2} I_{inj,31}^2,\ldots. \tag{13}$$

Since $I_{o,1}, I_{o,3},\ldots$ are the fundamental and harmonics of $I_o(t)$, we define the total output power of the oscillator (assume a 1Ω load)

$$I_o^2 = I_{o,1}^2 + I_{o,3}^2 + I_{o,5}^2 + \ldots. \tag{14}$$

The summation of the expressions in (13) yields

$$(\Delta\omega)^2 = \left[\left(\frac{\omega_o}{2Q_1}\right)^2 I_{inj,11}^2 + \left(\frac{\omega_o}{2Q_3}\right)^2 I_{inj,31}^2 + \ldots\right]\frac{1}{I_o^2}. \tag{15}$$

Define

$$\Delta\omega_{n1} = \left(\frac{\omega_o}{2Q_n}\right)\frac{I_{inj,n1}}{I_o}, \tag{16}$$

Eq.(15) can be written as

$$|\Delta\omega| = \sqrt{(\Delta\omega_{11})^2 + (\Delta\omega_{31})^2 + (\Delta\omega_{51})^2 + \ldots}. \tag{17}$$

Similarly, if the injection signal is a multi-tone, the output of the oscillator can be obtained by considering the effect of the harmonic components of the injection signal, i.e., $I_{inj,1}, I_{inj,3},\ldots$ individually. Utilizing (11) and (12), we have

$$I_o I_o^* = \frac{(I_{inj,11}^2 + I_{inj,13}^2 + I_{inj,11}I_{inj,13} + \ldots)\delta(\omega-\omega_{inj})}{\left[\frac{\partial H_{o,1}}{\partial\omega}\frac{\partial H_{o,1}^*}{\partial\omega}\right]_{\omega_o}(\Delta\omega)^2} + \frac{(I_{inj,31}^2 + I_{inj,33}^2 + I_{inj,31}I_{inj,33} + \ldots)\delta(\omega-3\omega_{inj})}{\left[\frac{\partial H_{o,3}}{\partial\omega}\frac{\partial H_{o,3}^*}{\partial\omega}\right]_{3\omega_o}(3\Delta\omega)^2} + \ldots \tag{18}$$

Matching the components that have the same frequency in (18) and summing each of components as (15) yields

$$(\Delta\omega)^2 = \left(\frac{\omega_o}{2Q_1}\right)^2 (I_{inj,11}^2 + I_{inj,13}^2 + I_{inj,11}I_{inj,13} + \ldots)\frac{1}{I_o^2} + \left(\frac{\omega_o}{2Q_3}\right)^2 (I_{inj,31}^2 + I_{inj,33}^2 + I_{inj,31}I_{inj,33} + \ldots)\frac{1}{I_o^2} + \ldots. \tag{19}$$

Define

$$\Delta\omega_n = \left(\frac{\omega_o}{2Q_n}\right)\frac{\sqrt{I_{inj,n1}^2 + I_{inj,n3}^2 + I_{inj,n1}I_{inj,n3} + \ldots}}{I_o}, \tag{20}$$

Eq.(19) can be written as

$$|\Delta\omega| = \sqrt{(\Delta\omega_1)^2 + (\Delta\omega_3)^2 + (\Delta\omega_5)^2 + \ldots}. \tag{21}$$

We comment on the preceding results: (i) Since the denominator of (16) is the total output current of the oscillator, Eq.(16) quantifies the contribution of $I_{inj,n1}$ to the overall lock range of the oscillator. (ii) Although the injection signal is a single-tone, it affects all harmonic oscillators. This is evident in (17). (iii) If the oscillator under injection is an ideal LC oscillator, $|\Delta\omega| = |\Delta\omega_{11}|$ as $\Delta\omega_{n1} = 0$ for n = 3, 5, ..., revealing that non-harmonic oscillators have a larger lock range as compared with harmonic oscillators. (iv) From (17) and (21), $\Delta\omega_{n1}$ for single-tone is evidently smaller than $\Delta\omega_n$ for multi-tone injections. (v) A comparison of (16), (17), (20), and (21) reveals that the lock range of non-harmonic oscillators with a multi-tone injection is larger as compared with that with a single-tone injection. The larger lock range is due to the contribution of the harmonics of the injection signal to each of the harmonic oscillators representing the non-harmonic oscillator. (vi) Although $H_{o,n}$ plays a critical role in analysis of non-harmonic oscillators, the final expression of the lock range of non-harmonic oscillators do not involve $H_{o,n}$. Only Q_n is needed.

3. Example

In this section we use the relaxation oscillator shown in Fig 3 to verify the theoretical findings presented earlier. The oscillator is designed in IBM 130 nm 1.2V CMOS technology and oscillates at 13 MHz. All devices are in sub-threshold to minimize power consumption. It is analyzed using Spectre from Cadence Design Systems with BSIM4 device models. The oscillator with (i) a sinusoid injection signal: $i_{inj}(t) = I_{inj}\sin(\omega_{inj}t)$, (ii) a dual-sinusoid injection signal: $i_{inj}(t) = I_{inj}\sin(\omega_{inj}t) + I_{inj}/3\sin(3\omega_{inj}t)$, and (iii) a square-wave injection signal (multi-tone) is analyzed. Fig.4 shows the spectrum of the oscillator in both unlocked and locked states. When the oscillator is unlocked, its spectrum contains multiple frequency components. When it is locked, only a single frequency component exists. The spectrum of the oscillator is therefore used to determine whether the oscillator is in lock or not.

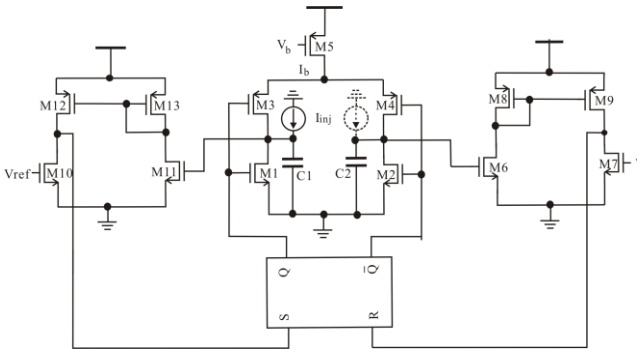

Figure 3: Schematic of relaxation oscillator with injection-locking. Circuit parameters: $W_{1,2,6,7,10,11}$ = 0.5µm, $W_{3,4}$ = 1.2µm, $W_{8,9,12,13}$ = 1.25 µm, W_5 = 2 µm, V_{ref} = 310 mV, I_b=253 nA, V_b = 620 mV.

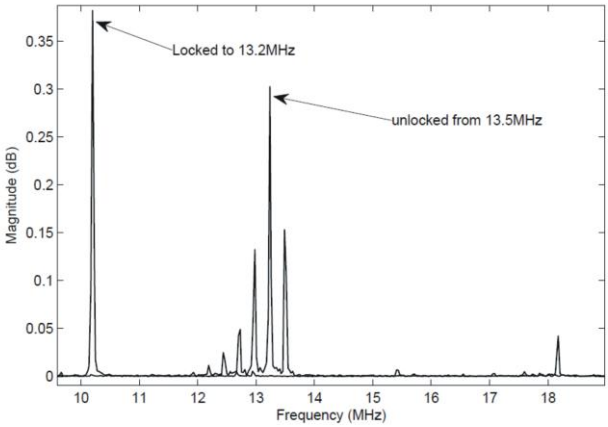

Figure 4: Simulated spectrum of the oscillator in lock state. The spectrum of the oscillator in the lock state is left-shifted by 3 MHz for a better view. I_{inj} = 12.65 nA and I_o = 126.5 nA, i.e. injection ratio=0.1.

Fig.5 investigates the dependence of the lock range on the strength of the injection signal. It is seen that increasing injection signal strength yields a larger lock range. Also observed is that single-tone injection gives the smallest lock range while square-wave injection (multi-tone) yields the largest lock range.

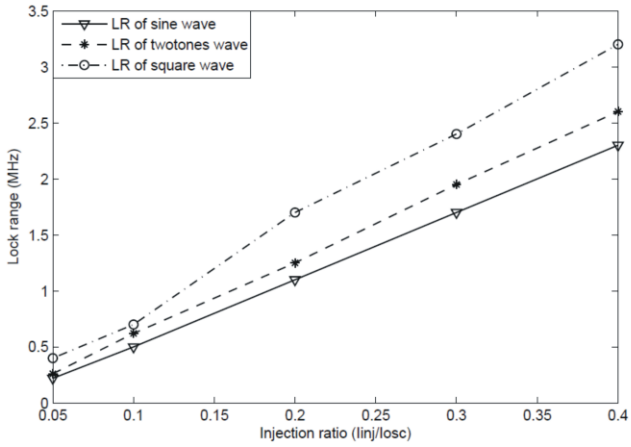

Figure 5: Simulated dependence of lock range (LR) of relaxation oscillator on injection strength and the number of frequency components of the injection signal.

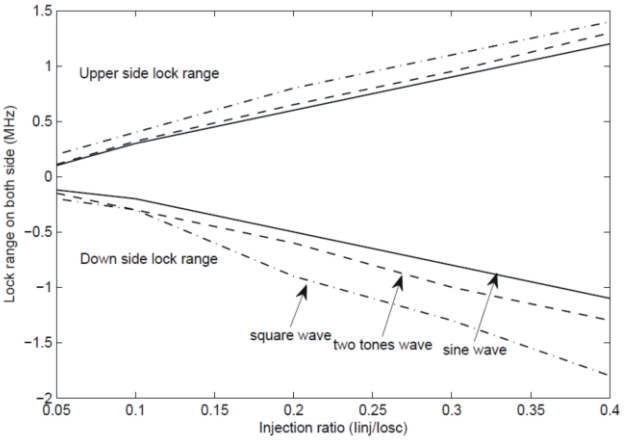

Figure 6: Asymmetry of lock range of relaxation oscillator.

When injection strength rises, the asymmetry of the lock range will become severe. This is evident in Fig.6 where the positive lock range ($\omega_{inj} > \omega_o$) and negative lock range ($\omega_{inj} < \omega_o$) are compared. The asymmetry of lock range is due to the nonlinear characteristics of non-harmonic oscillators [9]. In the theoretical results given in the paper, only first-order approximation that gives a symmetrical lock range is considered. When high-order terms are considered, the lock range asymmetry can be captured.

4. Conclusions

We have presented a general frequency-domain treatment of the lock range of non-harmonic oscillators. By representing non-harmonic oscillators with a set of harmonic oscillators, the intrinsic relation between the lock range of harmonic oscillators and that of non-harmonic has been obtained. We have shown that non-harmonic oscillators with a multi-tone injection exhibit a larger lock range as compared with that with a single-tone injection. The findings have been validated using a sub-threshold relaxation oscillator designed in IBM 130 nm 1.2 V CMOS technology.

5. Acknowledgement

Financial support from Natural Science and Engineering Research Council (NSERC) of Canada and computer-aided tools from CMC Microsystems, Kingston, Ontario, Canada are gratefully appreciated by the authors.

6. References

[1] F. Yuan, *CMOS Circuits for Passive Wireless Microsystems*, Springer, New York, 2010.

[2] *EPC radio-frequency identity protocols class-1 generation-2 UHF RFID protocol for communications at 860 MHz - 960 MHz, version 1.0.9*, EPCglobal Inc., 2005.

[3] N. Soltani and F. Yuan, "Non-harmonic injection-locked phase-locked loops with applications in remote frequency calibration of passive wireless transponders," *IEEE Trans. on Circuits and Systems I – Regular Papers*, Vol. 57, No. 12, pp.2381-2393, Sept. 2010.

[4] B. Razavi, "A study of injection locking and pulling in oscillators," *IEEE J. Solid-State Circuits*, Vol. 39, No. 9, pp. 1415-1424, Sept. 2004.

[5] B. Razavi, "A study of phase noise in CMOS oscillators," *IEEE J. Solid- State Circuits*, Vol. 31, No. 3, pp. 331-343, Mar. 1996.

[6] Y. Zhou and F. Yuan, "A study of lock range of injection-locked CMOS active-inductor oscillators using a linear control system approach," *IEEE Trans. on Circuits and Systems II – Express Briefs*, Vol. 58, No. 10, pp. 627-631, Oct. 2011.

[7] X. Lai and J. Roychowdhury, "Capturing oscillator injection locking via nonlinear phase-domain macromodels," *IEEE Trans. on Microwave Theory and Techniques*, Vol.52, No. 9, pp. 2251-2261, Sept. 2004.

[8] P. Maffezzoni, "Computing the synchronization regions of injection-locked strongly nonlinear oscillators for frequency division applications," *IEEE Trans. on Computer-Aided Design*, Vol.29, No. 12, pp. 1849-1858 Dec. 2010.

[9] S. Shekhar, M. Mansuri, F. O'Mahony, G. Balamurugan, J.E. Jaussi, J.Kennedy, D. J. Allstot, R. Mooney and B. Casper, "Strong injection locking in low-Q LC oscillators: modeling and application in a forwarded-clock I/O receiver," *IEEE Trans. on Circuits and Systems I – Regular Papers*, Vol. 56, No. 8, pp.1818-1829, Aug. 2009.